*Int. J. Solids Structures*, 1971, Vol. 7, pp. 913 to 930. Pergamon Press. Printed in Great Britain

# A LAMINATE COMPOSITE WITH A CRACK NORMAL TO THE INTERFACES†

P. D. HILTON‡ and G. C. SIH§

Lehigh University, Bethlehem, Pennsylvania

**Abstract**—The redistribution of stresses in a laminate composite due to the presence of a crack or flaw situated normal to the bond lines is studied. The many-layered composite is idealized to the case of a single layer of dissimilar material containing a crack which is sandwiched between two other layers of infinite height. The elastic properties of the two outer layers are assumed to be averaged properties over a large number of layers. Using the integral transform technique, the problem is formulated in terms of integral equations and solved for the singular stress field near the crack tip. The effects of crack size, layer height and the material properties of the composite on the stress-intensity factor are illustrated graphically. Presumably, this factor can be used to characterize the strength of a composite in the same way as it has been applied successfully to the single phase material within the framework of the linear theory of fracture mechanics.

Calculations are also carried out for approximating the stress-intensity factors for a crack inclined at an arbitrary position in the sandwiched layer. This is accomplished by taking the two extreme cases of a crack parallel and normal to the interfaces as the upper and lower bound solutions depending upon the relative stiffness of the layers.

## INTRODUCTION

A COMPOSITE being a man-made structure inherently contains some sort of imperfections in the form of either small voids or cracks. Any one of these flaws when it reaches a certain size can have a significant influence on the load transfer behavior within the composite. Generally speaking, it is the local intensification of the stresses around the dominant flaw that triggers fracture and often leads to failure of the system. Hence, it is essential to include pre-existing flaws in the strength analysis of composites.

The aim in composite studies of an analytical nature [1–3] is to provide, in a fundamental way, a set of mathematical formulas relating the influencing parameters of the composite in the pre-failure state. In an analysis, which accounts for pre-existing flaws, these parameters include the composite geometry, the flaw size, the level of applied load and the properties of the material. The relationships derived would presumably provide a better insight into the modes of fracture of composites. Solutions based on analysis of this type have been shown to agree with experimental data for metals. This concept of failure, known as "fracture mechanics", should apply equally well to non-metallic materials such as composites. Needless to say, the degree of success in applying the theory of fracture [4, 5] depends largely upon the accuracy achieved in the theoretical analysis. In a multiphase material, this task is made more difficult as a result of the complexity of the composite geometry.

† Research sponsored by the U.S. Air Force under Contract F33615-69-G-1417 through the Air Force Materials Laboratory at Wright-Patterson Air Force Base.

‡ Assistant Professor of Mechanics.

§ Professor of Mechanics.

For this reason, simplifying assumptions have often to be introduced to make the analysis manageable.

In this study, the composite geometry consists of a cracked layer of material bonded between two half-planes of different elastic properties. Both ends of the crack are located at an equal distance away from the interfaces which are aligned normal to the crack plane. The method of solution utilizes the displacement expressions derived by Sneddon [6], dealing with a crack in a finite width strip and follows that used by the authors in a previous paper [7] on a similar problem in which the crack is placed parallel to the bond lines. Numerical results for the stress-intensity factors are obtained from a standard Fredholm integral equation of the second kind and plotted against the ratio of the elastic moduli of neighboring layers for various values of the layer height to crack length ratio. An approximate solution for the more general situation where the crack is directed at an arbitrary angle to the interface is also discussed.

There is an analogous problem in cylindrical coordinates which consists of a penny-shaped crack contained in an infinite solid cylinder that is surrounded by and bonded to an infinite body of a second material. This penny-shaped crack problem can be formulated in much the same manner as the laminate problem considered here by making use of the corresponding displacement function for the cylinder which can be found in reference [6]. The analysis of this problem has not yet been attempted by the authors so there can be no assurance that later difficulties will not arise.

## FORMULATION OF PROBLEM

Assuming plane strain conditions, the laminate composite in Fig. 1 is made of a single layer of width $2h$ with shear modulus $\mu_1$ and Poisson's ratio $\nu_1$ bonded to two half-planes having elastic properties $\mu_2$ and $\nu_2$. A crack of length $2a(a < h)$ is centered along the $x$-axis as shown in Fig. 1. Symmetrical normal tractions and skew-symmetric shear tractions are

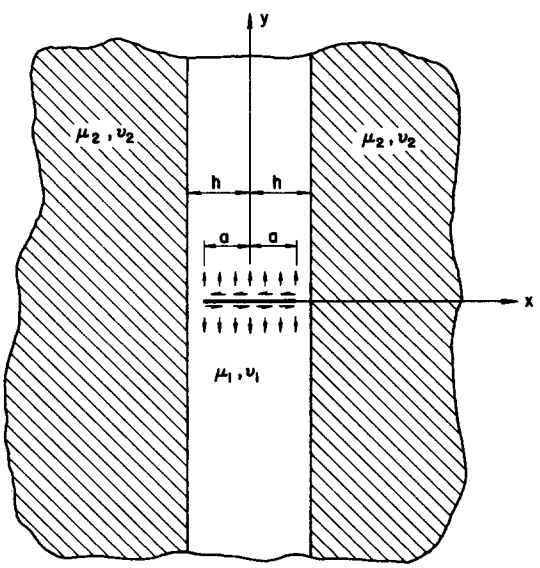


FIG. 1. Layer composite with a crack subjected to normal and shear tractions.

applied to the crack surfaces. In the following, the subscripts 1 and 2 will be used to refer the layer and surrounding half-planes, respectively.

The solutions within the layer will be required to satisfy matching conditions along $x = \pm h$ and mixed boundary conditions on the $x$-axis. A solution with sufficient generality to meet these conditions can be written as the superposition of the well known transform solutions [7] for a strip of width $2h$ centered on the $y$-axis and a half plane whose edge coincides with the $x$-axis. The resulting form which is assumed for the displacement field within the layer is:

$$\begin{aligned}
u_1 &= -\sqrt{(2/\pi)}\int_0^\infty \left\{\frac{1}{\eta}[f_1(\eta)-(1-2\nu_1)g_1(\eta)]\begin{bmatrix}\sinh(\eta x)\\ \cosh(\eta x)\end{bmatrix}+xg_1(\eta)\begin{bmatrix}\cosh(\eta x)\\ \sinh(\eta x)\end{bmatrix}\right\} \\
&\quad \begin{Bmatrix}\cos(\eta y)\\ \sin(\eta y)\end{Bmatrix} d\eta - \sqrt{(2/\pi)}\int_0^\infty \frac{\phi_1(\xi)}{\xi}(1-2\nu_1-\xi y)\,e^{-\xi y}\begin{bmatrix}\sin(\xi x)\\ -\cos(\xi x)\end{bmatrix} d\xi \\
v_1 &= \sqrt{(2/\pi)}\int_0^\infty \left\{\frac{1}{\eta}[f_1(\eta)+2(1-\nu_1)g_1(\eta)]\begin{bmatrix}\cosh(\eta x)\\ \sinh(\eta x)\end{bmatrix}+xg_1(x)\begin{bmatrix}\sinh(\eta x)\\ \cosh(\eta x)\end{bmatrix}\right\} \\
&\quad \begin{Bmatrix}\sin(\eta y)\\ -\cos(\eta y)\end{Bmatrix} d\eta + \sqrt{(2/\pi)}\int_0^\infty \frac{\phi_1(\xi)}{\xi}(2-2\nu_1+\xi y)\,e^{-\xi y}\begin{bmatrix}\cos(\xi x)\\ \sin(\xi x)\end{bmatrix} d\xi
\end{aligned} \tag{1}$$

for the normal and shear loading problems, respectively. Symmetry arguments are used to allow consideration of only the first quadrant with appropriate boundary conditions along the coordinate axes. Additionally, the layer solutions are required to match those for a half plane of the second material along $x = h$; namely,

$$\begin{aligned}
u_2 &= \sqrt{(2/\pi)}\int_0^\infty \eta[f_2(\eta)+g_2(\eta)\eta x+(1-2\nu_2)g_2(\eta)]\,e^{-\eta x}\begin{bmatrix}\cos(y\eta)\\ \sin(y\eta)\end{bmatrix} d\eta \\
v_2 &= \sqrt{(2/\pi)}\int_0^\infty \eta[f_2(\eta)+g_2(\eta)\eta x-2(1-\nu_2)g_2(\eta)]\,e^{-\eta x}\begin{bmatrix}\sin(y\eta)\\ -\cos(y\eta)\end{bmatrix} d\eta
\end{aligned} \tag{2}$$

for normal and shearing tractions, respectively.

## NORMAL LOADING

For normal loading, the boundary conditions along the $y$ and $x$-axes are

$$\begin{aligned}
(\sigma_{xy})_1(0, y) &= 0 \\
u_1(0, y) &= 0 \\
(\sigma_{xy})_1(x, 0) &= 0 \quad \text{for } |x| \le h; \qquad (\sigma_{xy})_2(x, 0) = 0 \quad \text{for } |x| \ge h \\
(\sigma_y)_1(x, 0) &= -p(x) \quad \text{for } |x| < a \\
v_1(x, 0) &= 0 \quad \text{for } a < |x| \le h; \qquad v_2(x, 0) = 0 \quad \text{for } |x| \ge h.
\end{aligned} \tag{3}$$

The matching conditions along $x = h$ are

$$\begin{aligned}
u_1(h, y) &= u_2(h, y) \\
v_1(h, y) &= v_2(h, y) \\
(\sigma_x)_1(h, y) &= (\sigma_x)_2(h, y) \\
(\sigma_{xy})_1(h, y) &= (\sigma_{xy})_2(h, y).
\end{aligned} \tag{4}$$

The stresses within the layer as obtained from the assumed displacement field (1) are

$$\frac{(\sigma_x)_1}{2\mu_1} = -\sqrt{(2/\pi)}\int_0^\infty [f_1(\eta)\cosh(\eta x)+\eta x g_1(\eta)\sinh(\eta x)]\cos(\eta y)\,d\eta$$

$$-\sqrt{(2/\pi)}\int_0^\infty \phi_1(\xi)(1-\xi y)\,e^{-\xi y}\cos(\xi x)\,d\xi$$

$$\frac{(\sigma_y)_1}{2\mu_1} = \sqrt{(2/\pi)}\int_0^\infty \{[f_1(\eta)+2g_1(\eta)]\cosh(\eta x)+\eta x g_1(\eta)\sinh(\eta x)\}\cos(\eta y)\,d\eta$$

$$-\sqrt{(2/\pi)}\int_0^\infty \phi_1(\xi)(1+\xi y)\,e^{-\xi y}\cos(\xi x)\,d\xi$$

$$\frac{(\sigma_{xy})_1}{2\mu_1} = \sqrt{(2/\pi)}\int_0^\infty \{[f_1(\eta)+g_1(\eta)]\sinh(\eta x)+\eta x g_1(\eta)\cosh(\eta x)\}\sin(\eta y)\,d\eta$$

$$-\sqrt{(2/\pi)}y\int_0^\infty \xi\phi_1(\xi)\,e^{-\xi y}\sin(\xi x)\,d\xi.$$

Note that $u_1(0, y) = 0$ and $(\sigma_{xy})_1(0, y) = 0$ by choice of the assumed form for the solution. Also $(\sigma_{xy})_1(x, 0) = 0$.

It is further required that

$$v_1(x,0) = 2(1-\nu_1)\int_0^\infty \frac{\phi_1(\xi)}{\xi}\cos(\xi x)\,d\xi = 0 \quad \text{for } |x| > a \tag{5}$$

and

$$\frac{(\sigma_y)_1(x,0)}{2\mu_1} = -\frac{d}{dx}\left\{\sqrt{(2/\pi)}\int_0^\infty \frac{\phi_1(\xi)}{\xi}\sin(\xi x)\,d\xi\right\} + \sqrt{\frac{2}{\pi}}\int_0^\infty \{[f_1(\eta)+2g_1(\eta)]\cosh(\eta x)$$

$$+\eta x g_1(\eta)\sinh(\eta x)\}\,d\eta = \frac{-p(x)}{2\mu_1} \quad \text{for } x < a. \tag{6}$$

Equation (5) is satisfied identically by the integral representation for $\phi_1(\xi)$:

$$\phi_1(\xi) = \sqrt{\frac{\pi}{2}}\xi\int_0^a t\psi_1(t)J_0(\xi t)\,dt \tag{7}$$

where $J_0(t)$ is the Bessel function of order zero. Substitution of (7) into (6) gives

$$\frac{d}{dx}\int_0^x \frac{t\psi_1(t)\,dt}{\sqrt{(x^2-t^2)}} - \sqrt{\frac{2}{\pi}}\int_0^\infty \{[f_1(\eta)+2g_1(\eta)]\cosh(\eta x)+\eta x g_1(\eta)\sinh(\eta x)\}\,d\eta$$

$$= \frac{p(x)}{2\mu_1} \qquad 0 \le x \le a. \tag{8}$$

This equation can be regarded as an Abel integral equation for $\psi_1(t)$ which, with the following identities

$$\int_0^t \frac{\cosh(\eta u)\,du}{\sqrt{(t^2-u^2)}} = \frac{\pi}{2}I_0(\eta t), \qquad \int_0^t \frac{u\sinh(\eta u)\,du}{\sqrt{(t^2-u^2)}} = \frac{\pi}{2}tI_1(\eta t)$$

is inverted to give

$$\psi_1(t) = \frac{2}{\pi}\int_0^t \frac{p(x)\,dx}{2\mu_1\sqrt{(t^2-x^2)}} + \sqrt{\frac{2}{\pi}}\int_0^\infty \{[f_1(\eta)+2g_1(\eta)]I_0(\eta t)+\eta t g_1(\eta)I_1(\eta t)\}\,d\eta$$

$$\text{for } 0 \le t \le a. \tag{9}$$

Here, $I_0(\eta t)$ and $I_1(\eta t)$ are the modified Bessel functions of order zero and one respectively.

The stress field in the half plane which results from the assumed displacement field (2) is

$$\frac{(\sigma_x)_2}{2\mu_2} = -\sqrt{(2/\pi)}\int_0^\infty \eta^2[f_2(\eta)+g_2(\eta)\eta x]\,e^{-\eta x}\cos(\eta y)\,d\eta$$

$$\frac{(\sigma_y)_2}{2\mu_2} = \sqrt{(2/\pi)}\int_0^\infty \eta^2[f_2(\eta)+g_2(\eta)\eta x-2g_2(\eta)]\,e^{-\eta x}\cos(\eta y)\,d\eta$$

$$\frac{(\sigma_{xy})_2}{2\mu_2} = -\sqrt{(2/\pi)}\int_0^\infty \eta^2[f_2(\eta)+g_2(\eta)\eta x-g_2(\eta)]\,e^{-\eta x}\sin(\eta y)\,d\eta. \tag{10}$$

This field automatically satisfies the conditions along $y = 0$.

The matching conditions on the interface $x = h$, from equation (4), become

1. $$-\frac{\mu_2}{\mu_1}\eta^2[f_2(\eta)+g_2(\eta)\eta h]\,e^{-\eta h} = -f_1(\eta)\cosh(\eta h)-\eta h g_1(\eta)\sinh(\eta h) - \frac{4\eta^2}{\pi}\int_0^\infty \frac{\xi\phi_1(\xi)}{(\eta^2+\xi^2)^2}\cos(\xi h)\,d\xi$$

2. $$-\frac{\mu_2}{\mu_1}\eta^2[f_2(\eta)+g_2(\eta)\eta h-g_2(\eta)]\,e^{-\eta h} = [f_1(\eta)+g_1(\eta)]\sinh(\eta h) + \eta h g_1(\eta)\cosh(\eta h)-\frac{4\eta}{\pi}\int_0^\infty \frac{\xi^2\phi_1(\xi)\sin(\xi h)}{(\eta^2+\xi^2)^2}\,d\xi$$

3. $$\eta\{f_2(\eta)+g_2(\eta)\eta h+[1-2\nu_2]g_2(\eta)\}\,e^{-\eta h} = -[f_1(\eta)-(1-2\nu_1)g_1(\eta)]\sinh(\eta h) - h g_1(\eta)\cosh(\eta h)-\frac{4}{\pi}\int_0^\infty \left[\frac{\eta^2-\nu_1(\eta^2+\xi^2)}{(\eta^2+\xi^2)}\right]\phi_1(\xi)\sin(\xi h)\,d\xi \tag{11}$$

4. $$\eta\{f_2(\eta)+g_2(\eta)\eta h-2[1-\nu_2]g_2(\eta)\}\,e^{-\eta h} = [f_1(\eta)+2(1-\nu_1)g_1(\eta)]\cosh(\eta h) + h g_1(\eta)\sinh(\eta h)+\frac{4}{\pi}\int_0^\infty \left[\frac{2\eta\xi^2+\eta^3-\nu_1(\xi^2+\eta^2)}{\xi(\eta^2+\xi^2)^2}\right]\phi_1(\xi)\cos(\xi h)\,d\xi.$$

The unknowns $f_2(\eta)$ and $g_2(\eta)$ are eliminated, thus reducing these four equations to two equations for $f_1(\eta)$ and $g_1(\eta)$ in terms of $\phi_1(\xi)$, i.e.

$$f_1(\eta) = c_{1j}(\eta)D_j(\eta) \qquad g_1(\eta) = c_{2j}(\eta)D_j(\eta) \tag{12}$$

where

$$c_{1j} = [\alpha_4(\eta)d_{1j}-\alpha_2(\eta)d_{2j}]/[\alpha_4(\eta)\alpha_1(\eta)-\alpha_3(\eta)\alpha_2(\eta)]$$

$$c_{2j} = -[\alpha_3(\eta)d_{1j}-\alpha_1(\eta)d_{2j}]/[\alpha_4(\eta)\alpha_1(\eta)-\alpha_3(\eta)\alpha_2(\eta)]$$

with the $\alpha_j$ and $d_{ij}$ defined as

$$d_{11} = \frac{4}{\pi}\left[\frac{\mu_1}{\mu_2}(1-2\nu_2)+\nu_1\right], \qquad d_{12} = -\frac{4\eta}{\pi}\left[2\frac{\mu_1}{\mu_2}(1-\nu_2)\right]$$

$$d_{13} = \frac{4\eta^2}{\pi}(1-\nu_1), \qquad d_{14} = 0$$

$$d_{21} = -\frac{4}{\pi}\left[2\frac{\mu_1}{\mu_2}(1-\nu_2)\right], \qquad d_{22} = \frac{4\eta}{\pi}\left[\frac{\mu_1}{\mu_2}(1-2\nu_2)+(2-\nu_1)\right]$$

$$d_{23} = 0, \qquad d_{24} = \frac{4\eta^3}{\pi}(1-\nu_1)$$

$$\alpha_1(\eta) = \left\{\frac{\mu_1}{\mu_2}[\cosh(\eta h)+(1-2\nu_2)\,e^{\eta h}]-\sinh(\eta h)\right\}/\eta$$

$$\alpha_2(\eta) = \left\{\frac{\mu_1}{\mu_2}[\eta h\sinh(\eta h)+(1-2\nu_2)(\sinh(\eta h)+\eta h\,e^{\eta h})]\right.$$

$$\left.-(1-2\nu_1)\sinh(\eta h)+\eta h\cosh(\eta h)\right\}/\eta$$

$$\alpha_3(\eta) = \left\{\frac{\mu_1}{\mu_2}[\cosh(\eta h)-2(1-\nu_2)\,e^{\eta h}]-\cosh(\eta h)\right\}/\eta$$

$$\alpha_4(\eta) = \left\{\frac{\mu_1}{\mu_2}[\eta h\sinh(\eta h)-2(1-\nu_2)(\sinh(\eta h)+\eta h\,e^{\eta h})]\right.$$

$$\left.-2(1-\nu_1)\cosh(\eta h)+\eta h\sinh(\eta h)\right\}/\eta.$$

The $D_j$ in equations (12) represent the following integral expressions:

$$D_1(\eta) = \int_0^\infty \frac{\xi^2\phi_1(\xi)\sin(\xi h)}{(\eta^2+\xi^2)^2}\,d\xi$$

$$D_2(\eta) = \int_0^\infty \frac{\xi\phi_1(\xi)\cos(\xi h)}{(\eta^2+\xi^2)^2}\,d\xi$$

$$D_3(\eta) = \int_0^\infty \frac{\phi_1(\xi)\sin(\xi h)}{(\eta^2+\xi^2)^2}\,d\xi \qquad (13)$$

$$D_4(\eta) = \int_0^\infty \frac{\phi_1(\xi)\cos(\xi h)}{\xi(\eta^2+\xi^2)^2}\,d\xi.$$

Using the integral representation for $\phi_1(\xi)$, equation (7), equations (13) may be rewritten in terms of the function $\psi_1(u)$ as

$$\begin{aligned}
D_1(\eta) &= -\left(\frac{\pi}{2}\right)^{\frac{1}{2}}\frac{1}{\eta}\int_0^a u\psi_1(u)\frac{\partial^3 m(\eta,u,h)}{\alpha h^3}\,du = \int_0^a \psi_1(u)L_1(\eta,u)\,du \\
D_2(\eta) &= \left(\frac{\pi}{2}\right)^{\frac{1}{2}}\frac{1}{\eta}\int_0^a u\psi_1(u)\frac{\partial^2 m(\eta,u,h)}{\alpha h^2}\,du = \int_0^a \psi_1(u)L_2(\eta,u)\,du \\
D_3(\eta) &= \left(\frac{\pi}{2}\right)^{\frac{1}{2}}\frac{1}{\eta}\int_0^a u\psi_1(u)\frac{\partial m(\eta,u,h)}{\alpha h}\,du = \int_0^a \psi_1(u)L_3(\eta,u)\,du \\
D_4(\eta) &= -\left(\frac{\pi}{2}\right)^{\frac{1}{2}}\frac{1}{\eta}\int_0^a u\psi_1(u)m(\eta,u,h)\,du = \int_0^a \psi_1(u)L_4(\eta u)\,du
\end{aligned} \tag{14}$$

in which

$$\begin{aligned}
m(\eta,u,h) &= -\frac{1}{\pi}\frac{\partial}{\partial\eta}\left\{\eta^2\int_0^\infty \frac{\cosh(\xi h)J_0(\xi u)}{\xi^2(\xi^2+\eta^2)}\,d\xi\right\} \\
&= \frac{1}{2}\frac{e^{-\eta h}}{\eta^2}\{(1+\eta h)I_0(\eta u)+\eta u I_1(\eta u)\}.
\end{aligned} \tag{15}$$

Now we make the substitutions for $f_1(\eta)$ and $g_1(\eta)$ in the integral equation (9). The revised equation is

$$\psi_1(t) = \frac{2}{\pi}\int_0^t \frac{p(x)}{2\mu_1\sqrt{(t^2-x^2)}}\,dx + \sqrt{\frac{2}{\pi}}\int_0^\infty \{(c_{1j}+2c_{2j})D_j(\xi)I_0(\xi t)+\xi t c_{2j}D_j(\xi)I_1(\xi t)\}\,dt. \tag{16}$$

A change in order of integration reduces this to the following Fredholm integral equation for $\psi_1(t)$:

$$\psi_1(t)+\int_0^a \psi_1(u)K(t,u)\,du = \frac{2}{\pi}\int_0^t \frac{p(x)}{2\mu_1\sqrt{(t^2-x^2)}}\,dx \tag{17}$$

where,

$$K(t,u) = \sqrt{(2/\pi)}\int_0^\infty \sum_{j=1}^{4}\{(c_{1j}+2c_{2j})L_j(\eta,u)I_0(\eta t)+\eta t c_{2j}L_j(\eta,u)I_1(\eta t)\}\,d\eta. \tag{18}$$

The kernel $K(t,u)$ can be further simplified by writing

$$L_j(\eta,u) = M_{j0}I_0(\eta u)+M_{j1}I_1(\eta u), \qquad j = 1,4$$

where

$$\begin{aligned}
M_{10} &= \frac{1}{2}\left(\frac{\pi}{2}\right)^{\frac{1}{2}} u\,e^{-\eta h}(2-\eta h), & M_{20} &= \frac{1}{2}\left(\frac{\pi}{2}\right)^{\frac{1}{2}} u\,e^{-\eta h}(1-\eta h)/\eta \\
M_{30} &= -\frac{1}{2}\left(\frac{\pi}{2}\right)^{\frac{1}{2}} u\,e^{-\eta h}h/\eta, & M_{40} &= \frac{1}{2}\left(\frac{\pi}{2}\right)^{\frac{1}{2}} u\,e^{-\eta h}(1+\eta h)/\eta \\
M_{11} &= \frac{1}{2}\left(\frac{\pi}{2}\right)^{\frac{1}{2}} u^2\eta\,e^{-\eta h}, & M_{21} &= \frac{1}{2}\left(\frac{\pi}{2}\right)^{\frac{1}{2}} u^2\,e^{-\eta h} \\
M_{31} &= -\frac{1}{2}\left(\frac{\pi}{2}\right)^{\frac{1}{2}} u^2\,e^{-\eta h}/\eta & M_{41} &= -\frac{1}{2}\left(\frac{\pi}{2}\right)^{\frac{1}{2}} u^2\,e^{-\eta h}/\eta^2.
\end{aligned} \tag{19}$$

Then,

$$K(t,u) = \sqrt{\frac{2}{\pi}}\int_0^\infty \sum_{j=1}^{4} \{(c_{1j}+2c_{2j})M_{j0}I_0(\eta u)I_0(\eta t) + (c_{1j}+2c_{2j})M_{j1}I_0(\eta u)I_1(\eta t)+\eta t c_{2j}M_{j0}I_1(\eta u)I_0(\eta t) + \eta t c_{2j}M_{j1}I_1(\eta u)I_1(\eta t)\}\,d\eta. \tag{20}$$

The Fredholm integral equation for $\psi_1(t)$ will be solved numerically for the case of uniform pressure, i.e. $p(x) = p$. For this case, it is convenient to first perform the following non-dimensionalization.

Let

$$\psi_1(t) = \psi_1(ar) = \frac{p}{\sqrt{r}}\frac{\Psi_1(r)}{2\mu_1}. \tag{21}$$

The governing equation, in this notation, becomes

$$\Psi_1(r) = \sqrt{r}+\sqrt{(rq)}\int_0^\infty \Psi_1(q)K^*(r,q)\,dq \tag{22}$$

where $K^*(r,q) = K(r,q)/q$ which can be shown to be symmetric in $r$ and $q$.

## SHEAR LOADING

Again, consider only the first quadrant with the following boundary conditions

$$\begin{aligned} (\sigma_x)_1(0,y) &= 0 \\ v_1(0,y) &= 0 \\ (\sigma_y)_1(x,0) &= 0 \quad \text{for } |x| \le h; \qquad (\sigma_y)_2(x,0) = 0 \quad \text{for } |x| \ge h \\ (\sigma_{xy})_1(x,0) &= -q(x) \quad \text{for } |x| < a \\ u_1(x,0) &= 0 \quad \text{for } a < |x| \le h; \qquad u_2(x,0) = 0 \quad \text{for } |x| \ge h. \end{aligned} \tag{23}$$

These conditions lead to the integral equation for $\psi_1(t)$.

$$\frac{d}{dx}\int_0^x \frac{t\psi_1(t)}{\sqrt{(x^2-t^2)}}\,dt+\sqrt{(2/\pi)}\int_0^\infty \{[f_1(\eta)+g_1(\eta)]\cosh(\eta x) + \eta x g_1(\eta)\sinh(\eta x)\}\,d\eta = \frac{q(x)}{2\mu_1} \qquad 0 \le x \le a \tag{24}$$

which can be inverted to

$$\psi_1(t) = \frac{2}{\pi}\int_0^t \frac{q_1(x)}{2\mu_1\sqrt{(t^2-x^2)}}\,dx - \sqrt{\frac{2}{\pi}}\int_0^\infty \{[f_1(\eta)+g_1(\eta)]I_0(\eta t) + \eta t g_1(\eta)I_1(\eta t)\}\,d\eta \qquad 0 \le x \le a. \tag{25}$$

The solution for the layer is, as in the symmetric case, required to match that for the half plane. This leads to relations for $f_1(\eta)$ and $g_1(\eta)$ in terms of integrals of $\psi_1(u)$, i.e.

$$f_1(\eta) = b_{1j}(\eta)D_j(\eta)$$
$$g_1(\eta) = b_{2j}(\eta)D_j(\eta)$$

where,

$$b_{1j} = [\beta_4(\eta)e_{1j} - \beta_2(\eta)e_{2j}]/[\beta_4(\eta)\beta_1(\eta) - \beta_3(\eta)\beta_2(\eta)]$$
$$b_{2j} = -[\beta_3(\eta)e_{1j} - \beta_1(\eta)e_{2j}]/[\beta_4(\eta)\beta_1(\eta) - \beta_3(\eta)\beta_2(\eta)] \tag{26}$$

and

$$e_{11} = 0, \qquad e_{12} = -\frac{4\eta}{\pi}\left[\frac{\mu_1}{\mu_2}(1-2\nu_2)+\nu_1\right]$$
$$e_{13} = \frac{4\eta^2}{\pi}\frac{2\mu_1}{\mu_2}(1-\nu_2), \qquad e_{14} = \frac{4\eta^3}{\pi}(1-\nu_1)$$
$$e_{21} = \frac{4}{\pi}(1-\nu_1), \qquad e_{22} = -\frac{4\eta}{\pi}\frac{2\mu_1}{\mu_2}(1-\nu_2)$$
$$e_{23} = -\frac{4\eta^2}{\pi}\left[\frac{\mu_1}{\mu_2}(1-2\mu_2)+\mu_1\right]. \qquad e_{24} = 0$$

The quantities $\beta_j(\eta)$ are defined as

$$\beta_1(\eta) = \left\{\frac{\mu_1}{\mu_2}[\sinh(\eta h)+(1-2\nu_2)\,e^{\eta h}]+\cosh(\eta h)\right\}/\eta$$
$$\beta_2(\eta) = \left\{\frac{\mu_1}{\mu_2}[\eta h\cosh(\eta h)+(1-2\nu_2)(\cosh(\eta h)+\eta h\,e^{\eta h})]\right.$$
$$\left.-(1-2\nu_2)\cosh(\eta h)+\eta h\sinh(\eta h)\right\}/\eta$$
$$\beta_3(\eta) = \left\{\frac{\mu_1}{\mu_2}[-\sinh(\eta h)+2(1-\nu_2)\,e^{\eta h}]+\sinh(\eta h)\right\}/\eta$$
$$\beta_4(\eta) = \left\{\frac{\mu_1}{\mu_2}[-\eta h\cosh(\eta h)+2(1-\nu_1)(\cosh(\eta h)+\eta h\,e^{\eta h})]\right.$$
$$\left.+2(1-\nu_1)\sinh(\eta h)+\eta h\cosh(\eta h)\right\}/\eta.$$

From this point, the analysis is identical to that for the symmetric problem. The final integral equation is

$$\psi_1(t)+\int_0^a \psi_1(u)H(t,u)\,du = \frac{2}{\pi}\int_0^t \frac{q(x)}{2\mu_1\sqrt{(t^2-x^2)}}\,dx, \qquad 0 \le t \le a \tag{27}$$

where,

$$H(t,u) = \sqrt{\frac{2}{\pi}}\int_0^\infty \sum_{j=1}^{4}\{(b_{1j}+b_{2j})M_{j0}I_0(\eta u)I_0(\eta t)$$
$$+(b_{1j}+b_{2j})M_{j1}I_0(\eta u)I_1(\eta t)+\eta t b_{2j}M_{j0}I_1(\eta u)I_0(\eta t)$$
$$+\eta t b_{2j}M_{j1}I_1(\eta u)I_1(\eta t)\}\,d\eta.$$

Numerical results will be presented for $q(x) = q = \text{const}$. Performing the same type of non-dimensionalization (21) as for the symmetric case gives

$$\Psi_1(r) = \sqrt{r} - \sqrt{(rs)} \int_0^1 \Psi_1(s) H^*(r, s)\, ds \tag{28}$$

where $H^*(r, s) = H(r, s)/s$ which is again symmetric in $r$ and $s$.

## THE STRESS INTENSITY FACTOR

For the case of normal loading, the stress intensity is found from the definition

$$k_1 = \lim_{x \to a^+} \sqrt{[2(x-a)]}(\sigma_y)_1(x, 0) \tag{29}$$

where for $x \geq a$, $(\sigma_y)_1(x, 0)$ is determined from

$$\frac{(\sigma_y)_1(k, 0)}{2\mu_1} = \frac{d}{dx} \int_0^a \frac{t\psi_1(t)}{\sqrt{(x^2 - t^2)}}\, dt - \sqrt{(2/\pi)} \int_0^\infty \{[f_1(\eta) + 2g_1(\eta)] \cosh(\eta x) + \eta x g_1(\eta) \sinh(\eta x)\}\, d\eta. \tag{30}$$

The stress intensity factor for the shearing mode is given by

$$k_2 = \lim_{x \to a^+} \sqrt{[2(x-a)]}(\sigma_{xy})_1(x, 0) \tag{31}$$

where, for the skew-symmetric problem, $(\sigma_{xy})_1(x, 0)$ is obtained from

$$\frac{(\sigma_{xy})_1(x, 0)}{2\mu_1} = \frac{d}{dx} \int_0^a \frac{t\psi_1(t)}{\sqrt{(x^2 - t^2)}}\, dt + \sqrt{\frac{2}{\pi}} \int_0^\infty \{[f_1(\eta) + g_1(\eta)] \cosh(\eta x) + \eta x g_1(\eta) \sinh(\eta x)\}\, d\eta. \tag{32}$$

In both cases, the second terms are nonsingular at $x = a$, and thus do not contribute to the stress intensity factors. Therefore,

$$\begin{aligned} k_1 &= 2\mu_1 \sqrt{(a)} \psi_1(a) = \Psi_1(1) p \sqrt{(a)} \\ k_2 &= 2\mu_1 \sqrt{(a)} \psi_1(a) = \Psi_1(1) q \sqrt{(a)} \end{aligned} \tag{33}$$

where, $\Psi_1(1)$ is determined from equation (22) for the case of normal loading and from equation (28) for applied shearing tractions. In the case of a homogeneous material $\mu_1 = \mu_2$, $\Psi_1(1)$ for either loading takes the value of unity and $k_1$, $k_2$ reduce to their respective limiting values of $p\sqrt{a}$ and $q\sqrt{a}$.

The function $\Psi_1(1)$ has been calculated numerically for a range of the variables $\mu_1/\mu_2$, $\nu_1$, $\nu_2$ and $a/h$. Figure 2 contains plots of the stress intensity factor, normalized by the Griffith's solutions for a single material specimen of the same geometry, $(k_1/p\sqrt{a})$, against the ratio of the shear module $(\mu_2/\mu_1)$ for various values of $a/h$. These graphs are for normal loading with both material Poisson's ratios equal ($\nu_1 = \nu_2 = 0{\cdot}3$). The intensity factor increases as the relative shear modulus of the matrix to that of the layer $(\mu_2/\mu_1)$ decreases. This effect is amplified as the ratio of the crack length to layer thickness increases. Note that all curves go through the point (1, 1) representing the Griffith configuration for a single material plate. The same data is plotted against $a/h$ in Fig. 3. In the limit as $a/h$ approaches 1·0, $k/p\sqrt{a}$ approaches infinity for $\mu_2/\mu_1 < 1{\cdot}0$ and zero for $\mu_2/\mu_1 > 1{\cdot}0$. The limiting cases

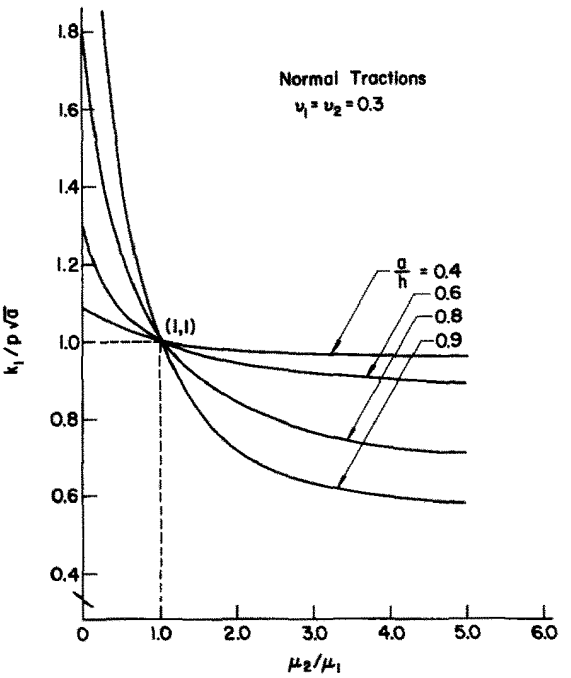


FIG. 2. Normalized stress-intensity factor $k_1$ vs. $\mu_2/\mu_1$ for $\nu_1 = \nu_2 = 0{\cdot}3$.

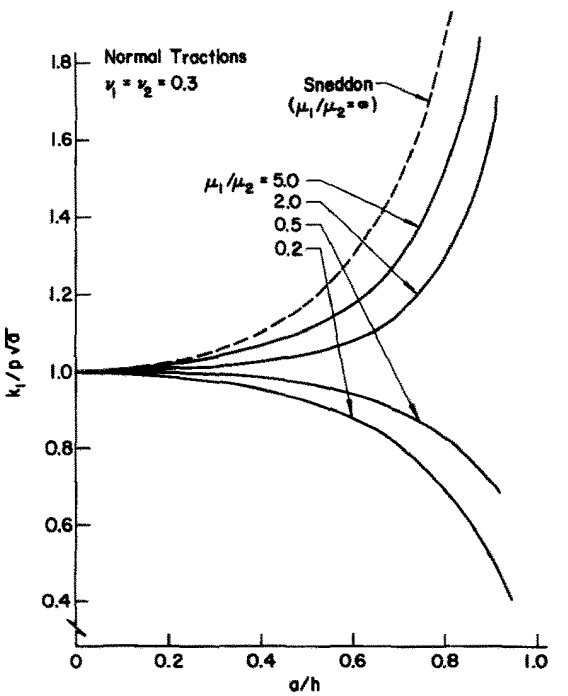


FIG. 3. Variation of $k_1/p\sqrt{a}$ with $a/h$ for $\nu_1 = \nu_2 = 0{\cdot}3$.

of $\mu_2/\mu_1 = 0, \infty$ have been calculated by Sneddon [6]. They represent a "stress-free" strip and a "constrained" strip, respectively.

The effect of different values of the Poisson's ratio for each constituent of the composite is demonstrated in Figs. 4–7. When the value of the Poisson's ratio for the layer is below that for the matrix, the graphs of $k_1/p\sqrt{a}$ against $\mu_2/\mu_1$ are shifted to the left, i.e. at $\mu_2/\mu_1 = 1{\cdot}0$ the normal stress intensity factor is less than 1·0. The opposite effect is observed when $\nu_2 < \nu_1$.

Results for the case of shearing tractions are presented in Figs. 8 and 9. Note that the same gross effects are observed.

## DISCUSSION OF RESULTS

Our purpose in solving this problem is to enable the prediction of failure for laminates in terms of the size and orientation of the "worst" flaw or crack within a layer of the composite. In general, the flaw or crack direction relative to the bond lines is unknown. Thus, for a given stress state, one would like to know the stress intensity factor for a crack of arbitrary angle. Failure prediction would then be based on the maximum value for the stress intensity factor associated with the "worst" crack angle.

Because of the lack of symmetry of the arbitrarily oriented crack problem, an analytical solution to the problem would be most difficult, if not impossible. However, valuable information can be gained from the knowledge of the solutions to the two extreme cases of a crack parallel to the bond lines (considered by the authors in a previous paper [7]) and one

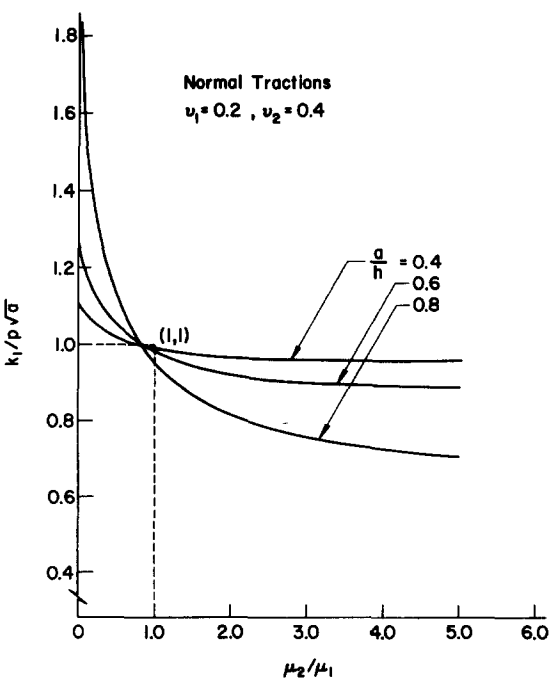


FIG. 4. Plot of $k_1/p\sqrt{a}$ vs. $\mu_2/\mu_1$ for $\nu_1 = 0{\cdot}2$ and $\nu_2 = 0{\cdot}4$.

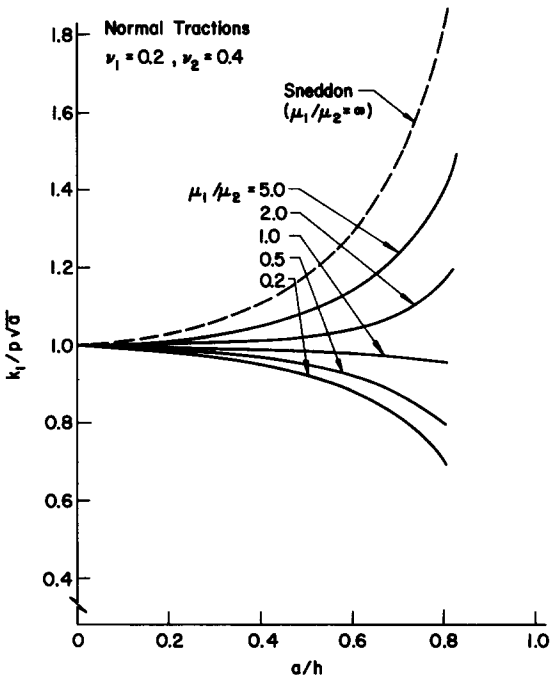


FIG. 5. Variation of $k_1/p\sqrt{a}$ with $a/h$ for $\nu_1 = 0{\cdot}2$ and $\nu_2 = 0{\cdot}4$.

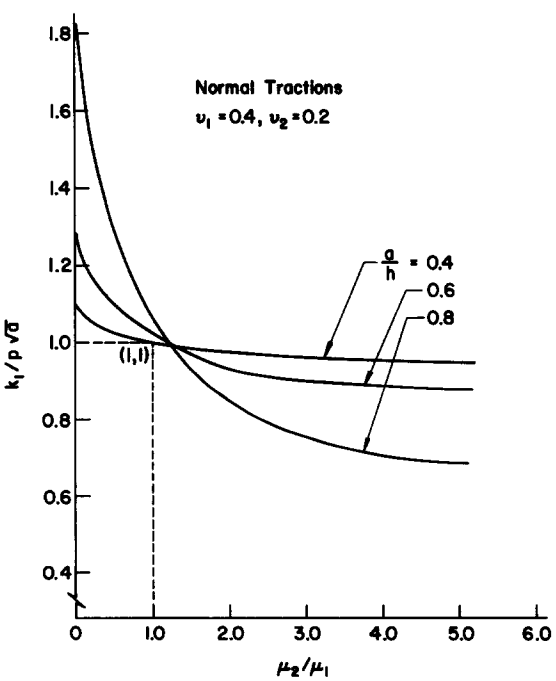


FIG. 6. Plot of $k_1/p\sqrt{a}$ vs. $\mu_2/\mu_1$ for $\nu_1 = 0{\cdot}4$ and $\nu_2 = 0{\cdot}2$.

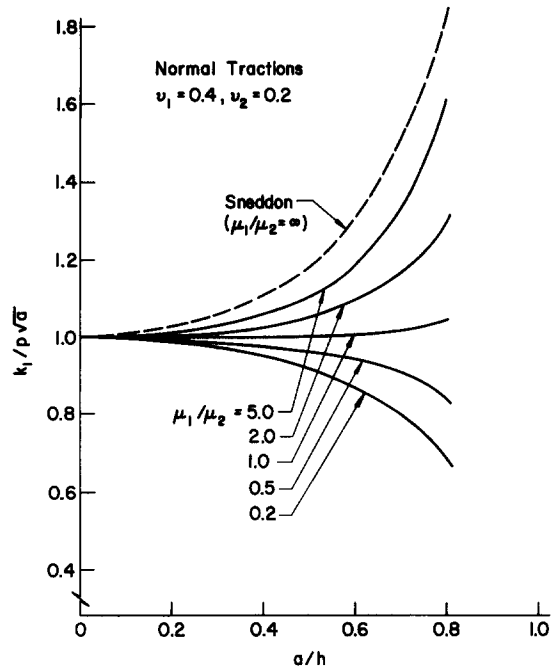


FIG. 7. Variation of $k_1/p\sqrt{a}$ with $a/h$ for $\nu_1 = 0{\cdot}4$ and $\nu_2 = 0{\cdot}2$.

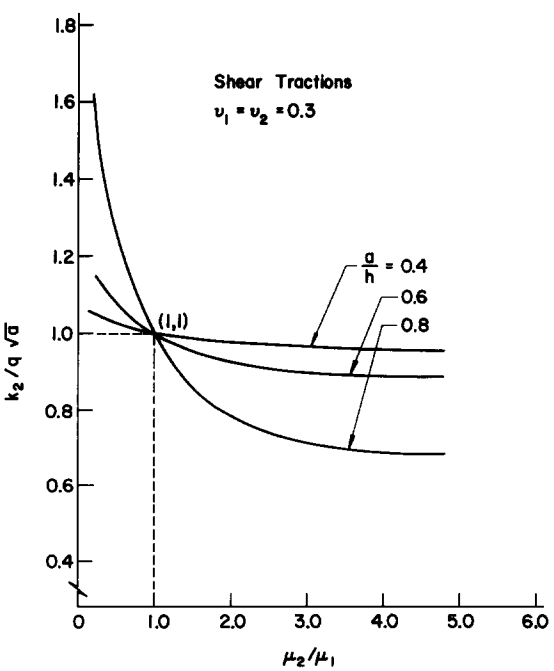


FIG. 8. Non-dimensionalized stress-intensity factor $k_2$ vs. $\mu_2/\mu_1$ for $\nu_1 = \nu_2 = 0{\cdot}3$.

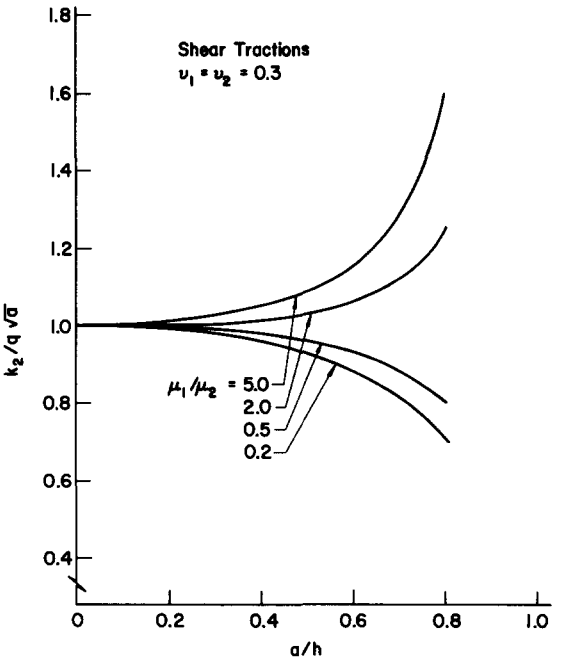


FIG. 9. Variation of $k_2/q\sqrt{a}$ with $a/h$ for $\nu_1 = \nu_2 = 0{\cdot}3$.

normal to them as dealt with here. For the case of normally applied tractions, the results for the two foregoing cases are displayed in Figs. 10 and 11 for a number of layer width to crack length ratios, $h/a$. For short cracks, i.e. $h/a \gg 1{\cdot}0$, the effect of the composite structure on a crack parallel to the material interface is more severe than on one normal to it. As the relative crack length increases, the influence of the bond lines on the crack tip for the normal crack appears to take over and the composite effect on this case becomes increasingly stronger than for the parallel crack. In the limit as $h/a$ approaches 1·0 the order of the stress singularity for the normal crack becomes dependent on the material properties and the problem has to be reformulated.

As mentioned earlier, it is not yet possible to get the solutions for a crack of intermediate angles to the bond lines; however, it is reasonable to anticipate that these results will lie between the two special cases. An approximate formula for cracks at intermediate angles which is based on Mohr's circle will be presented next.

Consider a line crack in an infinite region of one material, oriented at an angle $\alpha$ from the horizontal axis Fig. 12(a). For applied biaxial stress $\sigma_x^\infty$ and $\sigma_y^\infty$, the stress intensity factors are given by [4]

$$k_1(\alpha) = \left[\frac{\sigma_x^\infty + \sigma_y^\infty}{2} + \frac{\sigma_y^\infty - \sigma_x^\infty}{2}\cos 2\alpha\right]\sqrt{a}$$

$$k_2(\alpha) = \left[\frac{\sigma_y^\infty - \sigma_x^\infty}{2}\sin 2\alpha\right]\sqrt{a}. \tag{34}$$

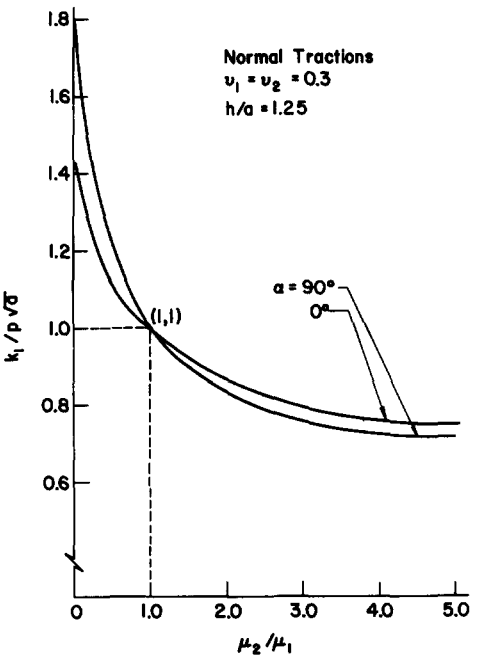


FIG. 10. Comparison of non-dimensionalized stress-intensity factor, $k_1/p\sqrt{a}$, for parallel and normal cracks at $h/a = 1{\cdot}25$.

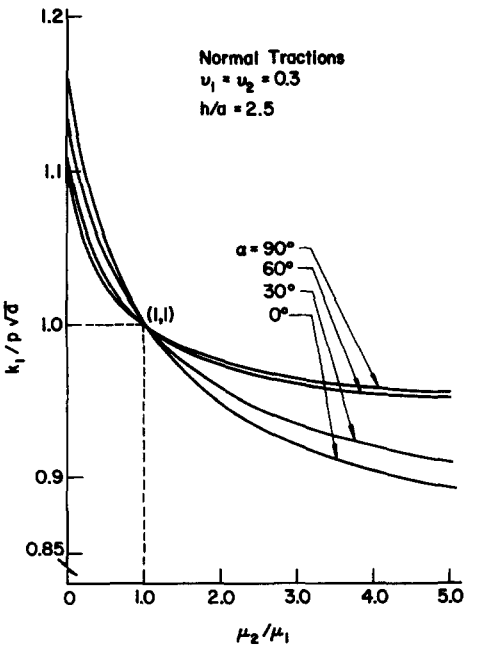


FIG. 11. Comparison of non-dimensionalized stress-intensity factor, $k_1/p\sqrt{a}$, for parallel and normal cracks at $h/a = 2{\cdot}5$.

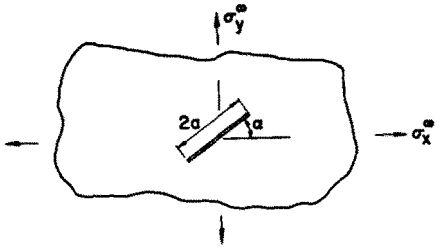


FIG. 12(a). Crack in an infinite, single material, plate subjected to biaxial tension.

These equations can be rewritten in the form

$$k_1(\alpha) = \frac{[k_1^{(1)}+k_1^{(2)}]}{2} + \frac{[k_1^{(1)}-k_1^{(2)}]}{2}\cos 2\alpha$$

$$k_2(\alpha) = \left|\frac{[k_1^{(1)}-k_1^{(2)}]}{2}\sin 2\alpha\right| \tag{35}$$

where $k_1^{(1)} = k_1(0°)$ and $k_1^{(2)} = k_1(90°)$.

This demonstrates that, for the single-material problem, it is sufficient to know the stress intensity factors for cracks oriented along two orthogonal planes and further that, with this knowledge, the Mohr's circle technique can be employed to find the stress intensity factor for a crack directed at any other angle to the loading.

Referring now to the problem of a crack in a layer between two half-planes of a second elastic material, Fig. 12(b), the values for the stress intensity factors have been presented for the cases of normal loading with the crack either parallel to [7] or perpendicular to the bond lines. An approximation for the stress intensity factors for a crack oriented α degrees from the bond lines, Fig. 12(b), is given by the Mohr's circle technique, i.e.

$$k_1(\alpha) = \frac{(k_1^{(1)}+k_1^{(2)})}{2} + \frac{(k_1^{(1)}-k_1^{(2)})}{2}\cos 2\alpha$$

$$k_2(\alpha) = \left|\frac{(k_1^{(1)}-k_1^{(2)})}{2}\sin 2\alpha\right| \tag{35}$$

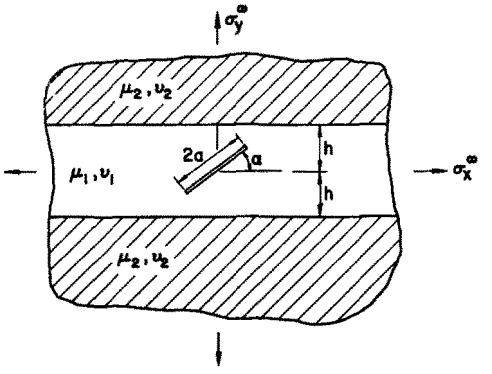


FIG. 12(b). Crack at arbitrary angle in a sandwiched layer subjected to biaxial tension.

where $k_1^{(1)}$ is the stress intensity factor for a crack parallel to the bond lines with normal pressure $p = \sigma_y^\infty$ and $k_1^{(2)}$ is that for a crack normal to the bond lines subjected to pressure $p = \sigma_x^\infty$. Typical results for $k_1(\theta)$ are shown in Fig. 11 for the case $p = \sigma_x^\infty = \sigma_y^\infty$ with $h/a = 2{\cdot}5$. A caution is required here. For a crack at arbitrary angle, $\alpha$, the normal and shear modes of failure are interdependent, thus, any meaningful fracture criteria must take into account both $k_1(\alpha)$ and $k_2(\alpha)$. Reference is made to [4].

Equations (35) are exact in the limit as $h/a$ approaches infinity for any material properties; as well as, for the special case $\mu_2/\mu_1 = 1$, $\nu_1 = \nu_2$. It is expected that their accuracy will decrease as the actual problem deviates increasingly from both these limiting cases. The range of applicability of these approximate equations is not yet known.

## REFERENCES

[1] J. R. RICE and G. C. SIH, Plane problems of cracks in dissimilar materials. *J. appl. Mech.* **32**, 418–423 (1965).
[2] A. B. PERLMAN and G. C. SIH, Elastostatic problems of curvilinear cracks in bonded dissimilar materials. *Int. J. Engng Sci.* **5**, 845–867 (1967).
[3] G. C. SIH, P. D. HILTON and R. P. WEI, Exploratory Development of Fracture Mechanics of Composite Systems, Technical Report AFML-TR-70-112 (1970).
[4] G. C. SIH and H. LIEBOWITZ, Mathematical Theories of Brittle Fracture, *Mathematical Fundamentals of Fracture*, edited by H. Liebowitz, Vol. 2, pp. 67–190. Academic Press (1968).
[5] G. R. IRWIN, Fracture, *Encyclopedia of Physics*, Vol. 6, pp. 551–590. Springer (1958).
[6] I. N. SNEDDON and M. LOWENGRUB, *Crack Problems in the Classical Theory of Elasticity*, pp. 62–72. Wiley (1969).
[7] P. D. HILTON and G. C. SIH, A Sandwiched Layer of Dissimilar Material Weakened by Crack-Like Imperfections, *Proceedings: Fifth Southeastern Conference on Theoretical and Applied Mechanics*, to be published.

(*Received* 20 *August* 1970; *revised* 8 *December* 1970)

**Абстракт**—Исследуется перераспределение напряжений в слоистом теле, вследствие наличия щели или дефекта, расположенного нормально к линиям ограничения. Много-слоистое тело идеализи руется для случая одиночного слоя из различного материала, содержающего щель. Этот слой находится между двумя слоями бесконечной высоты. Упругие свойства двух внешних слоев принимаются в смысле средних свойств больмого числа слоев. Пользуясь методом интегрального преобразования формулируется задача в интегральных уравнениях и решается для сингулярного поля напряжений, вблизи конца щели. Иллюстрируются, графически, эффекты размера щели, высоты слоя и свойств ма териала отдельных слоев на фактор интенсивности напряжений. Повидиму этот фактор можно использовать для характеристики сопротивления слоистых материалов темже путем, как принимается удачно для одно-фазового материала, в рамках линейной теории механики разрушения.

Проводятся расчеты для приближения факторов интенсивности напряжений для щели, расположенной на произвольной точке сандвичевых слоев. Это достигается путем использования двух экстремальных случаев щели параллельной и нормальной к поверхности раздела, как верзний и нижний предел решений, зависимых от относительной жесткости слоев.